A novel method for assessing adherent single-cell stiffness in tension: design and testing of a substrate-based live cell functional imaging device

Bartalena, G ; Grieder, R ; Sharma, R I ; Zambelli, T ; Muff, R ; Snedeker, J G

DOI: https://doi.org/10.1007/s10544-010-9493-3

Biomed Microdevices (2011) 13:291–301
DOI 10.1007/s10544-010-9493-3

A novel method for assessing adherent single-cell stiffness in tension: design and testing of a substrate-based live cell functional imaging device

Guido Bartalena · Reto Grieder · Ram I. Sharma · Tomaso Zambelli · Roman Muff · Jess G. Snedeker

Published online: 1 December 2010

Abstract Various micro-devices have been used to assess single cell mechanical properties. Here, we designed and implemented a novel, mechanically actuated, two dimensional cell culture system that enables a measure of cell stiffness based on quantitative functional imaging of cell-substrate interaction. Based on parametric finite element design analysis, we fabricated a soft (5 kPa) polydimethylsiloxane (PDMS) cell substrate coated with collagen-I and fluorescent micro-beads, thus providing a favorable terrain for cell adhesion and for substrate deformation quantification, respectively. We employed a real-time tracking system that analyzes high magnification images of living cells under stretch, and compensates for gross substrate motions by dynamic adjustment of the microscope stage. Digital image correlation (DIC) was used to quantify substrate deformation beneath and surrounding the cell, leading to an estimate of cell stiffness based upon the ability of the cell to resist the applied substrate deformation. Sensitivity of the system was tested using chemical treatments to both "soften" and "stiffen" the cell cytoskeleton with either 0.5 μg/ml Cytochalasin-D or 3% Glutaraldehyde, respectively. Results indicate that untreated osteosarcoma cells (SAOS-2) exhibit a 1.5±0.7% difference in strain from an applied target substrate strain of 8%. Compared to untreated cells, those treated with Cyochalasin-D passively followed the substrate (0.5±0.5%, $p<0.001$), whereas Glutaraldehyde enhanced cellular stiffness and the ability to resist the substrate deformation (2.9±1.6%, $p<0.001$). Nano-indentation testing showed differences in cell stiffness based on culture treatment, consistent with DIC findings. Our results indicate that mechanics and image analysis approaches do hold promise as a method to quantitatively assess tensile cell constitutive properties.

Keywords Biaxial stretching · Single live cell imaging · Feature tracking · Cell mechanics · Experiments · Modeling

G. Bartalena · R. Grieder · R. I. Sharma · R. Muff · J. G. Snedeker (✉)
Orthopedic Research Laboratory, University of Zurich, Balgrist, Forchstrasse 340,
CH-8008, Zurich, Switzerland
e-mail: snedeker@ethz.ch

G. Bartalena · R. I. Sharma · J. G. Snedeker
Institute for Biomechanics,
Department of Mechanical Engineering, ETH Zurich,
Wolfgang-Pauli-Strasse 10,
CH-8093, Zurich, Switzerland

T. Zambelli
Institute for Biomedical Engineering,
Department of Electrical Engineering, ETH Zurich,
Gloriastrasse 35,
CH-8092, Zurich, Switzerland

1 Introduction

Cell mechanical properties have attracted the interest of researchers from different fields (medicine, biology, bioengineering). In particular cell stiffness has emerged as one of the most interesting characteristics to study, as it is increasingly linked to various human disease states (Suresh et al. 2005; Suresh 2007). Pathologic changes in cellular functions are often manifested in the cytoskeleton, which enables cellular mechanical stability and functional behaviors like migration. In a variety of diseases reviewed by Lee et al. (Lee and Lim 2007), this complex biopolymer network undergoes structural alterations leading to change in cell stiffness. Malaria, for example, manifests a stiffening of erythrocytes, which can result in vessel occlusion, anemia, coma or even death (Lincoln et al. 2004). Many cancers are also known to be

associated with changes of cellular mechanical properties; in particular cancer cells have been demonstrated to be more deformable than healthy controls in melanoma (Ochalek et al. 1988), osteosarcoma (Docheva et al. 2008), and leukemia (Yao et al. 2003). Thus studying the "mechanical signature" of diseased cells may lead to a better understanding of the underlying pathology, and cell stiffness could represent a potentially useful biological marker for disease detection.

Various micro-engineered systems have been employed in the last decades to investigate single cell mechanical properties *in-vitro,* including platforms based upon nano-indentation (Cross et al. 2007; Patel et al. 2010), micro-fluidic optical stretching (Lincoln et al. 2007), SU-8 micro-tools (Wacogne et al. 2008), and traction force microscopy which infers cellular strains from the displacement of nanoreporters embedded in the substrate to indirectly quantifies cell-matrix force exchange (Munevar et al. 2001). While each approach can offer relative advantages, substrate based methods allow probing adherent cells with approximately physiological boundary conditions (substrate topology, ligand chemistry, substrate compliance).

While quantification of cell traction force using substrate based methods have been well described by others (Wang and Pelham 1998; Tan et al. 2003), the quantification of cell stiffness requires application of an external force to the cell, and a corresponding quantification of cellular deformation in response. Given the small footprint beneath the cell, tensile stretching of individual adherent cells is technically demanding, and schemes that allow larger cell substrates to be actuated while retaining the cell within a microscopic field of view have begun to emerge (Serrell et al. 2007; Wall et al. 2007; Gerstmair et al. 2009). However, until now these approaches have involved the application of non-homogenous substrate strains, and more importantly have failed to yield viable measures of cell stiffness. We propose a novel system that employs engineered cellular substrates fabricated from Polydimethylsiloxane (PDMS) that are specifically tuned to allow quantification of cell stiffness. The functional imaging platform we introduce is enabled by a real-time tracking system that allows high magnification imaging of the actively deformed substrate, and a localized measurement of single actuated cells. To our knowledge, this is the first device providing a stiffness measurement based upon substrate stretching, as well as the first that combines biaxial cell stretching with simultaneous live cell imaging. While the approach is described and validated in the context of non-patterned (non-stamped) PDMS substrates, such an approach could be eventually be translated to PDMS micro-devices (micro-channels, micro-wells), by mounting them to a commercially available substrate actuation system as we describe below.

2 Material and methods

2.1 Operating principle

We developed a novel functional imaging platform built around a modified commercial device that incorporates a tunable stiffness gel substrate to provide a controlled, homogenous, biaxial tensile strain to cultured cells. The system permits simultaneous imaging of a deforming cell at low (10X) or high magnification (40X). An active motion compensation algorithm tracks the movement of surface nano-reporters and moves the motorized microscope stage accordingly, simultaneously storing the image of the deformed substrate along with the corresponding actuation pressure. Digital image correlation is used to quantify substrate deformation beneath and surrounding the cell, allowing an estimate of cell stiffness based upon the ability of the cell to resist the applied substrate deformation

2.2 Finite element analysis of cell-substrate interaction

In order to guide platform design, parametric finite element simulations were conducted using a commercial software (Ansys V12.0, Ansys Inc.). The goal was to investigate the response of cell substrates of different elastic moduli (E) to both the applied base-membrane actuation and simulated cell resistance to the applied deformation.

Many different mechanical models of the cell have been implemented in the last decades to predict cellular response when subjected to external load and debate regarding the best way to do it remains ongoing (Lim et al. 2006; Krishnan et al. 2009). We implemented a simplified (mechanically isotropic) 3D representation of a single cell seeded on a PDMS substrate undergoing 8% strain (Fig. 1(a) and (b)). PDMS was modeled as an homogeneous and isotropic, linear elastic material (Masuda et al. 2008), with Poisson's ratio=0.4 and a range of E moduli. The cell was also assumed to be an isotropic elastic material with E=3.6 kPa (values obtained from AFM indentation tests—see below) and a Poisson's ratio of 0.37 (Shin and Athanasiou 1999). Beside the aforementioned E modulus, two further cell models with E=1 kPa and E= 10 kPa, respectively, were implemented, in order to study system sensitivity. Contacts between the two bodies ("focal adhesions") were assumed to be no-slip (glued node) and the base of the PDMS substrate was modeled as a frictionless support. Pressure was applied to the lateral faces of the substrate and set in order to produce a macroscopic 8% biaxial strain on its surface, under the assumption of finite deformation. Principal maximum strains were analyzed. Sensitivity analysis of the mesh was also performed in order to confirm the independence of the result from the mesh element size. Results from the finite element analysis were then used to guide the design of the cell substrate.

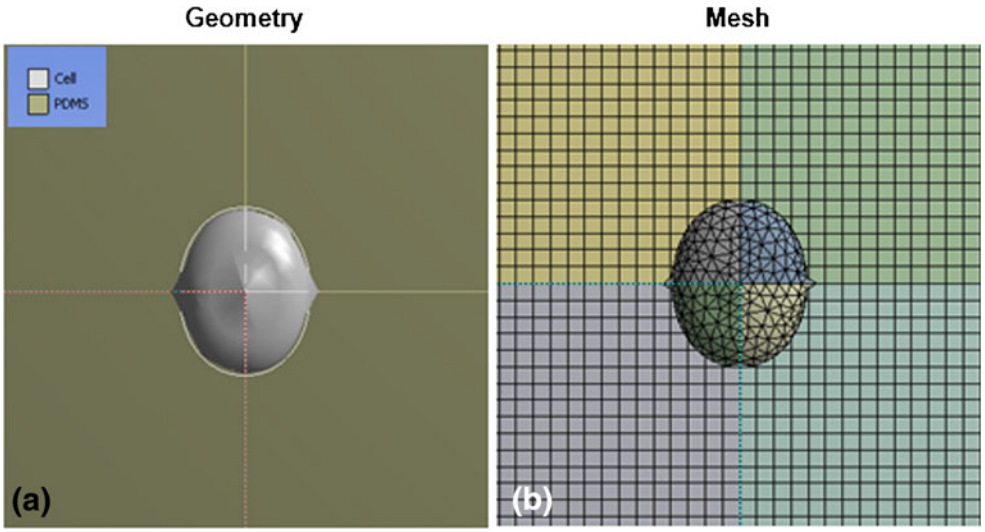

Fig. 1 (**a**) Geometry and (**b**) mesh of simplified representations of a cell on PDMS substrates, as modeled in the finite element analysis

2.3 Stretching device

We used a commercially available vacuum-actuator (StageFlexer, FlexerCell International, Hillsborough, North Carolina) (Fig. 2(a)), to apply equibiaxial strain (Wall et al. 2007; Bieler et al. 2009) to a silicone membrane (d=43 mm) by drawing it over a circular loading post (d=25 mm) lubricated with a silicone-based grease according to manufacturer recommendations. In a novel extension of this system, a highly elastic, interpositional polydimethylsiloxane (PDMS) gel was superimposed on the silicon membrane as described later in detail.

2.4 Cell substrate fabrication

Polydimethylsiloxane (PDMS) is a frequently used material to produce stretchable culture substrates. PDMS is biocompatible, shows excellent optical properties and it is stretchable to physiologically relevant ranges with an approximately linear material behavior (Wipff et al. 2009). Various base-to-curing agent ratios were tested in a tensile configuration using a universal tensile testing machine (Zwick 1456, Zwick GmbH) and elastic moduli were derived from the nominal stress/strain curves at quasi-static deformation speeds (data not shown).

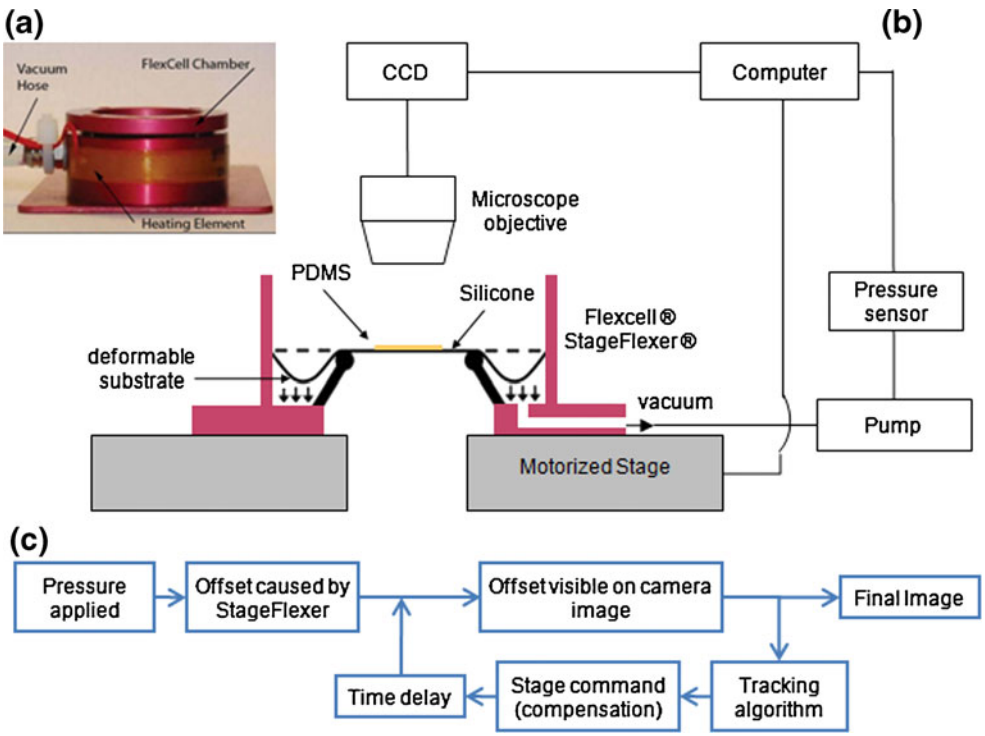

Fig. 2 (**a**) FlexCell® StageFlexer®. (**b**) Experimental set-up of the functional Imaging Platform. (**c**) Closed loop control system

After mixing ratio optimization, an interpositional substrate was cast onto the commercial silicone base membrane. In brief, the PDMS (Sylgard 184, Dow Corning) mixture was degassed for 30 min under vacuum, and then placed in an aluminum ring (d=25 mm) on the StageFlexer silicone membrane, giving the PDMS a desired shape. A controlled volume of PDMS was injected to the ring yielding a consistent thickness (500 μm; flatness verified by optical imaging at high magnification—all surface markers were verified to lie within the microscope depth of field, or 1 μm). Given its hydrophobic nature, PDMS requires surface treatments to allow binding extracellular matrix proteins like collagen that can provide a favorable terrain for cell adhesion and sufficient cell-matrix binding to prevent cell decoupling from the substrate (Wipff et al. 2009). Therefore the PDMS was plasma treated (Diener FEMTO, Nagold, Germany) for 30 s at low energy, making the PDMS hydrophilic. The substrate was then immersed in a solution of amino propyltriethoxysilane (APTES) (10% in ethanol) for 1 h at 45°C. The sample was copiously washed with sterile PBS and immersed in 3% Glutaraldehyde in PBS for 20 min before rinsing with sterile PBS (Tan and Desai 2004; Wipff et al. 2009). Collagen-I at 10 μg/ml was prepared from a stock solution along with 200 nm amine modified latex fluorescent beads (Invitrogen) diluted to 1:1000 and used as surface nano-reporters. This solution was then overlaid on the surface and incubated for 3 h at 37°C. Substrates were then washed three times with sterile PBS prior to cell culture.

2.5 Technical description of the functional imaging platform

The StageFlexer was mounted on a Nikon Eclipse E600 upright optical microscope, equipped with epi-fluorescence, a motorized X-Y stage (H101 Proscan II, Prior Scientific) and a CCD Camera (DX20, Kappa opto-electronics GmbH). All experiments were performed with a Nikon 40x lens with a 0.65 NA and a 1.0 μm field of depth. A custom-made electronic board with an integrated pressure sensor was used to automatically tag acquired camera image files with the applied pressure. The platform is illustrated schematically in Fig. 2(b).

We developed a computer vision algorithm based on phase correlation and used it to compute the offsets between subsequently acquired real-time digital images. Performance issues with convolution in the time domain were addressed by performing convolution in the frequency domain instead. However, obtained image correlation results were periodic, and produced two possible values for each offset in x and y direction. This ambiguity was resolved by taking the smaller of the two possible values, based on the assumption that the difference between two images could never be more than half the size of the image.

The image tracking procedure was implemented on a personal computer as a closed loop controller. This allowed the system to adapt to small changes such as stage offset imperfections or small delay time variance in all the components. However the effects of delay on the dynamics of the closed loop control system were quite severe. The largest delay times were caused by the camera, stage and tracking algorithms as illustrated in Fig. 2(c). These time delays were observed to cause serious system instability, which was compensated by taking into account the controller stage movements that had already been sent to the stage but were not yet visible on the image (Smith Predictor) (Foulkes and Miall 2000). Empirical testing showed that the imposed delay was approximately one control loop cycle, and incorporating the predicted offset effectively resolved system instability.

2.6 Image processing and strain field calculation

Several (6–8) high resolution (0.26 μm/pixel) images of speckled substrates (green channel) and cells (red channel) in a reference state and a deformed state, were taken using short term time lapse microscopy. A target vacuum pressure was preselected to supply a target strain of 8% to the membrane, according to calibration experiments (see below).

A custom algorithm designed in MATLAB (The MathWorks, Natick, MA) was used to derive the substrate strain field, based on micro-beads displacement following substrate stretch. The routine integrated an ImageJ plug-in (bUnwarpJ) that performed a simultaneous registration of the two images (reference and deformed) (Arganda-Carreras et al. 2006), producing a spline interpolated displacement field. We then calculated the two principal strains (equal to radial and circumferential strains in a 2D equibiaxial strain state) deriving the spatial gradient of the spline smoothed displacement field (Snedeker et al. 2006). Maximum principal strain was considered as an effective measure to account for both dilatational strains (stretching along the axes of the imaging plane) and distortional (shear) strains. Average values and standard deviation were determined within a designated region of interest (ca $300\times300\mu m^2$, depending on cell position and size) that was selected to include one or two cells.

2.7 System calibration

In order to calibrate our system, three original FlexCell silicone membranes were plasma-treated following the same protocol applied to the PDMS and fluorescent micro-beads were attached to their surface. Strain-pressure behaviors on the FlexCell Stageflexer were characterized following micro-beads displacement. We then performed

the same calibration experiment on three PDMS substrates fabricated as previously described. The goal was to verify that the strain was uniformly transferred throughout the thin PDMS substrate, thus characterizing its baseline behavior. Inter- and intra-membrane variations were also calculated and observed to confirm reproducibility and uniformity on the entire surface.

2.8 Cell culture and experiments

Human SAOS-2 (HTB-85) cells were obtained from the American Type Culture Collection (Rockville, MD, USA). Cells were cultured in Dulbecco's Modified Eagle's Medium (4.5 g/l glucose)/Ham (F12) (Invitrogen, Carlsbad, CA, USA), supplemented with 10% heat-inactivated fetal calf serum at 37°C in an atmosphere of 95% air and 5% CO_2.

Prior to the experiment, cells were pre-labeled with Vybrant Dil cell-labeling solution (Invitrogen), as per manufacturer recommendation. Samples were then seeded at 2000 cells/cm^2 and incubated for 6 h at 37°C before experimental characterization, so that they could reach a fully spread conformation (spreading kinetics data not presented). Substrates were then mounted on the platform and kept immersed under medium for the entire duration (~15 min/membrane) of the experiment, performed at room temperature.

Cells were treated biochemically to both "soften" and "stiffen" their cytoskeleton with either Cytochalasin-D (0.5 μg/ml in Medium) (Chou et al. 2009) or Glutaraldehyde (3% in PBS), respectively. The reagent was over laid for 30 min prior to image acquisition. In the case of cytochalasin D, polymerization of F-actin is inhibited leading to disruption of cytoskeleton and reduction of cell traction forces. Conversely, treating cells with Glutaraldehyde introduces chemical cross links that severely stiffen the cell (Hoh and Schoenenberger 1994).

2.9 Atomic force microscopy

AFM indentation was performed using a Nanowizard AFM (JPK Instruments, Berlin, Germany). Cells were seeded on PDMS (Sylgard 184, Dow Corning) substrates; PDMS was made in a 60:1 base-to-curing-agent ratio and functionalized following the same protocol used for the Flexcell experiments, in an attempt to create identical experimental conditions. All measurements were taken in medium and at room temperature. PLL-PEG-coated, silicon sphere (R= 1 μm) AFM tips (NanoWorld AG, Neuchâtel, Switzerland) were calibrated by measuring the free resonance frequency in air prior to the experiment, determining a spring constant of 0.42 N/m. The extension/retraction speed was set to 4 μm/s, while the maximum load was chosen individually for each experiment so that the indentation depth was small enough to avoid any influence of the underlying surface. Force-displacement curves of approximately 20 cells were taken and then analyzed with the JPK IP software that applied a Hertz model for spherical indentation in order to calculate cell stiffness (Dimitriadis et al. 2002; Darling et al. 2007).

3 Results

3.1 Finite element analysis of cell-substrate interaction

FE results predicted that cells ranging in stiffness from 1 to 10 kPa, cultured on relatively stiff substrates (100 kPa) cannot resist an applied substrate strain. This is indicated in Fig. 3 by the fact that the strain distribution on the substrate surface is not affected by the presence of the cell. Conversely, cells simulated on a soft substrate were able to resist active deformation, and indicated a lower substrate strain beneath the cell body. Furthermore the system was predicted to be able to discern different cell stiffness based on the drop in substrate strain beneath the cell body.

3.2 Cell substrate fabrication

A wide spectrum of base-to-curing-agent ratios was tested to characterize PDMS mechanical behavior under stretch. Figure 4(a) shows the tensile E moduli corresponding to the investigated mixing ratios. Based on these results and preliminary FEA results, a 60:1 ratio (corresponding to 4.7± 1.0 kPa elastic modulus) was selected and fabricated on the FlexCell silicone membrane, as described above. Homogeneity of the material was confirmed by uniformity of the resultant surface strain field, and by spherical indenation tests (data not shown).

Following the functionalization process, PDMS was tested again using the same tensile testing protocol. Tensile E modulus of functionalized PDMS was found equal to 5.3± 0.6 kPa, with no statistical difference ($p \geq 0.1$) in comparison to untreated PDMS (Fig. 4(b)).

Planarity of the fabricated substrates could be visually confirmed by the fact all beads within any given image were in focus, thus inferring that substrate height variation was less than 1 μm (the employed 40x lens, as previously described in the Methods, has a 1.0 μm field of depth). We used IHC with antibodies against the functionalizing ligand (Collagen-I) to provide verification that integrity of the ligand coated substrates was not disrupted by the stretching experiment (data not shown).

3.3 System calibration and performance

Calibration experiments indicated that the employed interpositional PDMS substrate could be reliably bonded to the

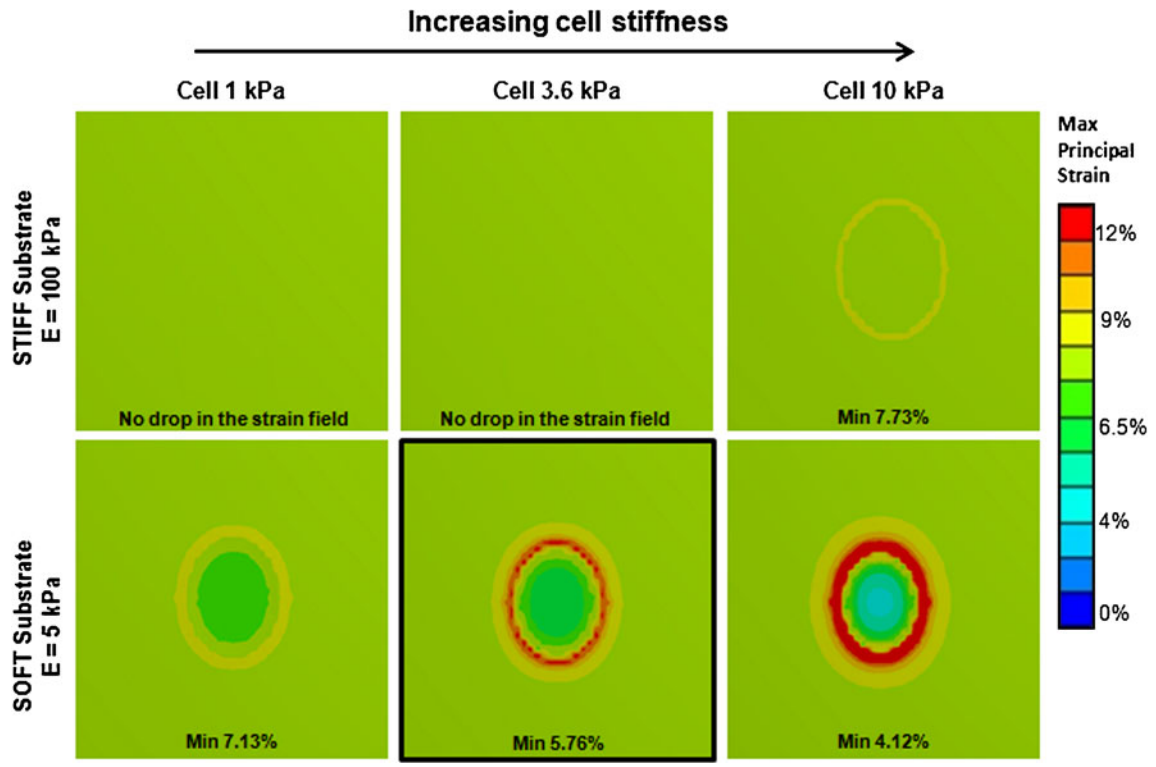

Fig. 3 FEA of substrates and cells of different compliances undergoing 8% strain. While on the moderately stiff substrate (100 kPa) the cell is not able to influence substrate deformation pattern and simply follows the applied strain, the soft substrate (5 KPa) is affected by cell resistance and shows a drop in the strain field underneath cell body. The black square highlights the model configured to replicate the configuration used in experiments

silicon membrane. Strain distribution on PDMS surface matched the StageFlexer Silicone membrane behavior, confirming that strain was consistently transferred throughout the substrate (see Fig. 5). Uniformity of the strain distribution on PDMS substrate (panel in Fig. 5, A=750× 750 μm^2) also indicated that no local debonding occured. Substrate-to-substrate variation and intra-substrate variation (Fig. 6(a) and (b), respectively) were found to be low, with both coefficients of variation less than 7% over an applied vacuum pressure increment from −400 hPa to −500 hPa.

Addition of culture medium, both with and without 3% Glutaraldehyde (as used to stiffen the cells), were demonstrated to not affect the magnitude or uniformity of the strain distribution (data not shown).

The tracking system and stage motion compensation algorithm allowed stretching the substrate up to 8% deformation within a few seconds (~5 s), at magnifications up to and including 40x. Minor z-focus adjustments were required to compensate for out-of-plane movements associated with thinning of the stretched membrane.

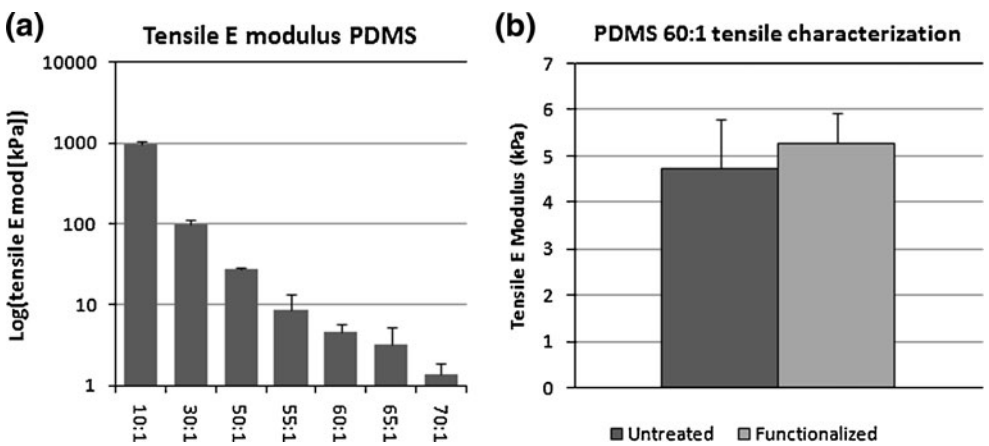

Fig. 4 (**a**) PDMS tensile E modulus characterization. The substrate elastic modulus was varied by changing the base-to-curing-agent ratio. (**b**) E Moduli comparison between "untreated" and "plasma-treated" 60:1 PDMS

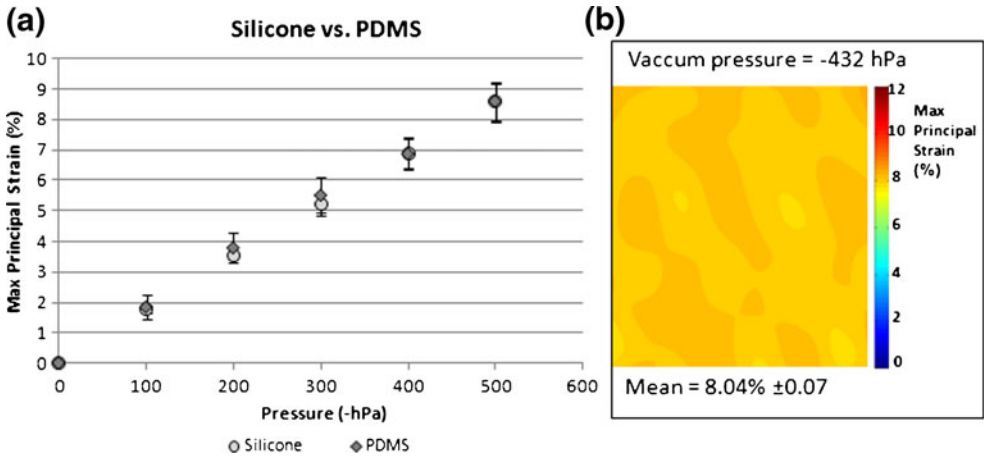

Fig. 5 (**a**) PDMS calibration showing substrate strain—actuator vacuum pressure points for three silicone membranes and three PDMS substrates, respectively pooled together. (**b**) Strain plot of PDMS being stretched to 8%, with no cells seeded

3.4 Cellular experiments

Fluorescently labeled SAOS-2 cells were seeded on the functionalized PDMS substrate and incubated for 6 h at 37°C. Figure 7 shows a typical result: following an applied substrate deformation of ~8%, the cell proved able to resist, exhibiting a drop from the applied substrate strain beneath the cell body and a consequently higher strain surrounding it. Average strain values of the deformed image were used as a baseline to calculate the strain drop caused by the cell. This maximum principal strain drop, as plotted in Fig. 7, allowed comparison of cells from different regions and on different membranes, thus facilitating interpretation of results.

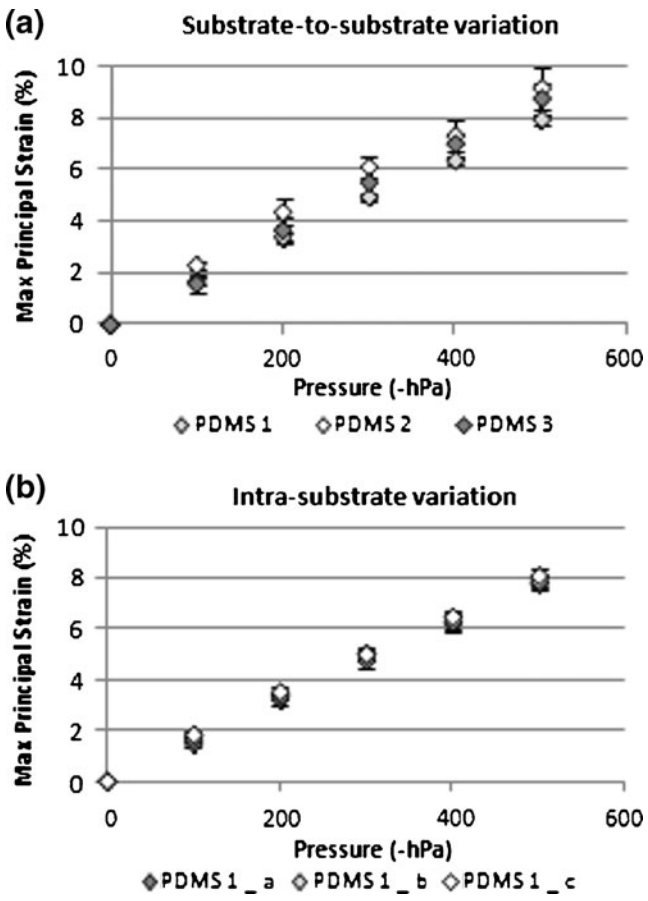

Fig. 6 PDMS surface strain calibration. (**a**) Substrate-to-substrate and (**b**) intra-substrate variations are shown

Individual cells (n=35) were evaluated from experiments on 6 different membranes. The mean principal strain drop from the applied substrate strain was quantified to be 1.5±0.7%.

In order to broadly test the sensitivity of the system with respect to cell stiffness, two experiments using cells treated with cytochalasin-D (CD) and two further experiments used glutaraldehyde (GA), as described above. The goal in the first case was to disrupt the cytoskeleton by inhibiting actin polymerization (Chou et al. 2009) and reduce cell's ability to resist to active deformation; and to crosslink it in the second case, thus making the cell stiffer (Hoh and Schoenenberger 1994). CD-treated cells produced an average drop from substrate deformation of only 0.5±0.5%, significantly different than untreated cells (p<0.001; Fig. 8). Conversely, glutaraldehyde increased the ability of cells to resist to substrate deformation up to 2.9±1.6% (p<0.001). These results demonstrate the capability of the platform to discern cells based on their stiffness.

4 AFM results

AFM testing (Fig. 9) yielded compressive moduli values of 4.33±2.19 kPa for untreated SAOS-2 cells. When treated with GA, cell modulus was dramatically increased to 68.7±20.7 kPa, while the CD treated cells showed significantly (p<0.05) lower compressive elastic modulus (2.96±1.16 kPa).

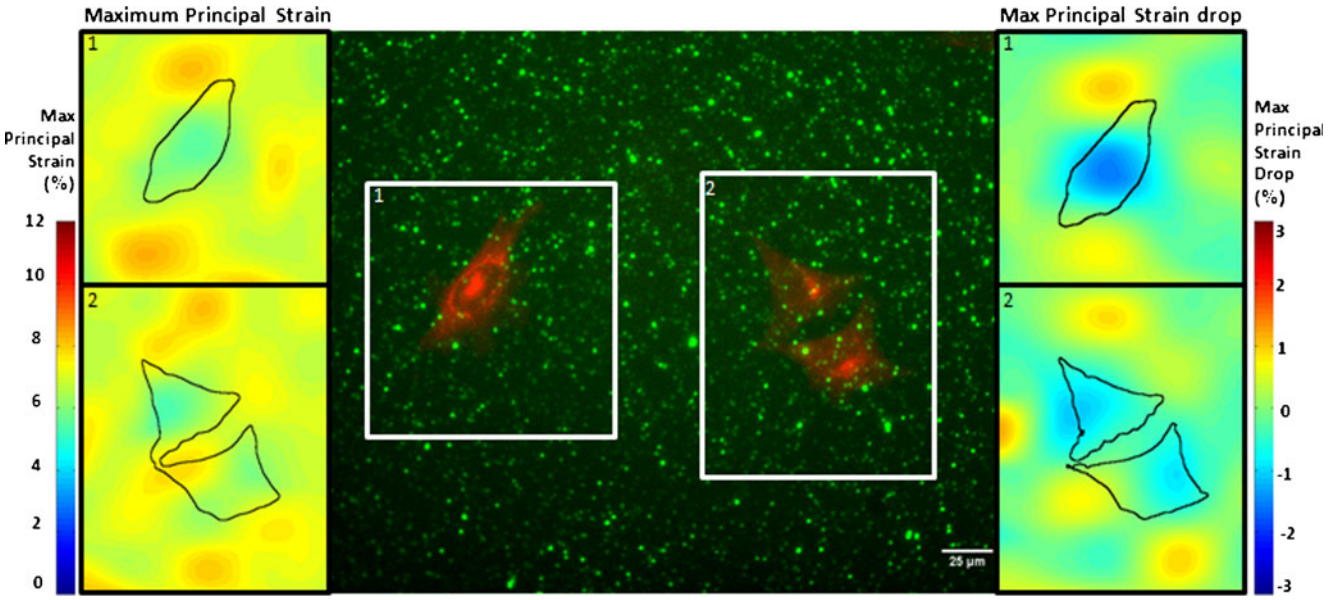

Fig. 7 Fluorescently labeled SAOS-2 cells seeded on a PDMS substrate functionalized with collagen-I and fiducial microbead markers (*central image*). Maximum principal strain plot (*left-hand side*) and maximum principal strain drop plot (*right-hand side*) of the selected areas of the same substrate undergoing ~8% deformation. Segmented cell borders are superimposed

5 Discussion

Cell stiffness represents a potentially promising biological marker to characterize certain disease states, since many diseased cells undergo cytoskeletal alterations and changed mechanical properties. Various single-cell techniques, such as AFM indentation (Cross et al. 2007; Cross et al. 2008), stretching by optical tweezers (Guck et al. 2005), micropi-

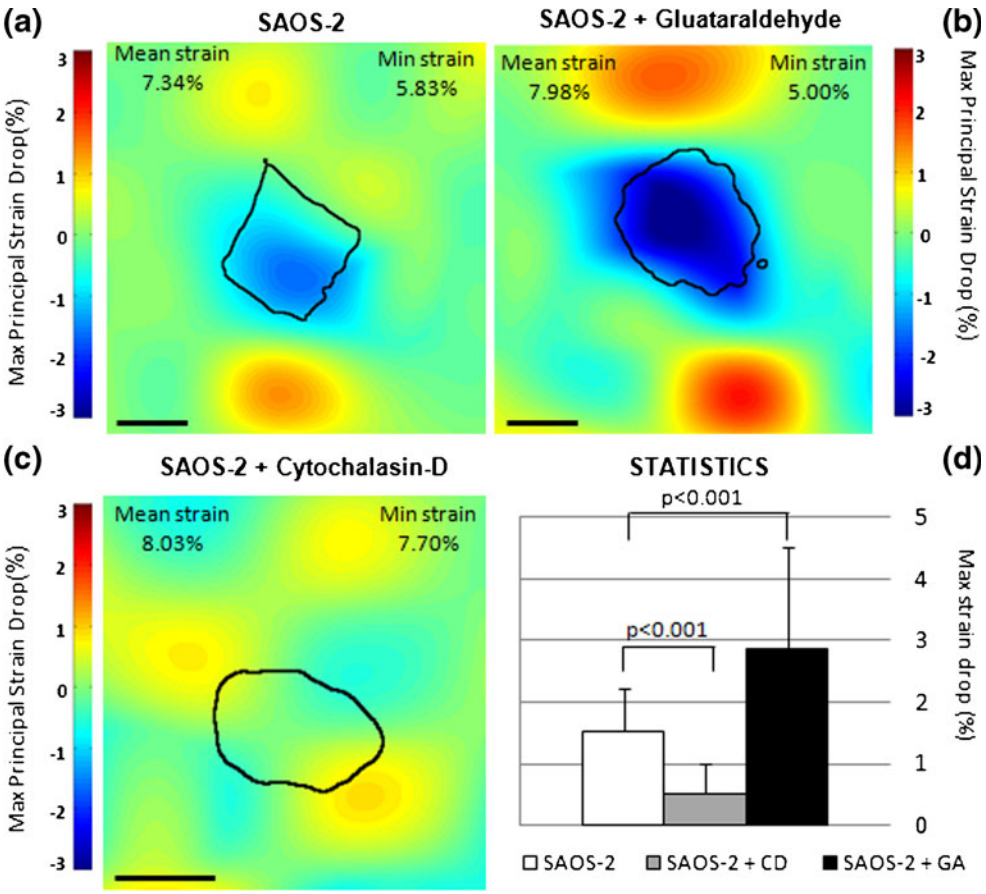

Fig. 8 (**a**–**c**) Maximum principal strain drop plot of SAOS-2 in three different conditions (Normal, Cytochalasin-D treatment, Glutaraldehyde treatment) seeded on a functionalized PDMS substrate undergoing 8% deformation and respective statistics. (Scale bar=25 µm) (**d**) Summary of the results relative to the three conditions

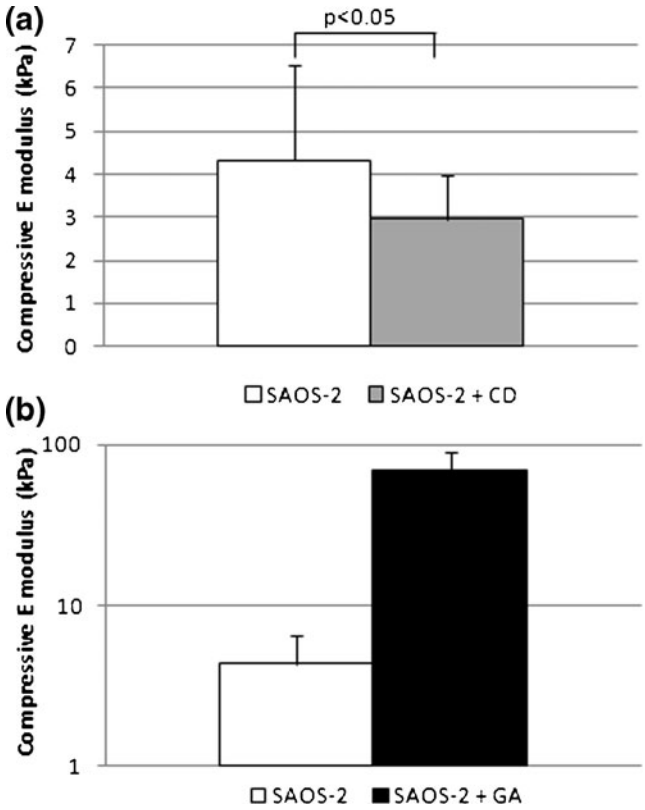

Fig. 9 AFM results. Panel A shows the compressive E modulus of normal SAOS-2 with respect to SAOS-2 treated with Cytochalasin ($p<0.05$). Panel B shows a comparison with Glutaraldehyde treated cells ($p<0.001$)

pette aspiration (Paulitschke and Nash 1993) and others, have been implemented and used to measure this parameter. However, these approaches generally fail to mimic cell tensions imposed on adherent cells by a stretching matrix. An *in vitro*, substrate-based stretching assay of cell stiffness, while still removed from the physiological situation of a cell embedded in a three dimensional matrix, nevertheless loads cytoskeletal structures in a fundamentally different manner compared to more common approaches, and can thereby yield additional/ complementary information.

In the present study we developed and characterized a substrate-based cell stiffness assay, measuring cellular ability to resist to active deformation on "sufficiently soft" substrates. In order to explore and expand this concept, a finite element analysis of the system was performed. This demonstrated that cells cultured on relatively stiff substrates (100 KPa) simply follow the applied deformation, whereas cells were predicted to be able to resist if seeded on a soft substrate (5 KPa). Therefore standard commercially available actuated silicone membranes (StageFlexer) were considered unsuitable for our purposes, and PDMS was introduced as an interpositional substrate, because of its highly tunable stiffness, ability to be bonded to the base silicone membrane, and potential for eventual embedding of patterned micro-devices.

While earlier studies have characterized the commercial device to provide a well controlled biaxial strain (Vande Geest et al. 2004), the novel configuration of our system including an interpositional substrate required further characterization. We were able to demonstrate that the cell substrate strain was consistently and uniformly transferred through the PDMS substrate, as indicated by consistent and uniform PDMS surface strain patterns. The platform development was completed with a dynamic tracking system that allowed high magnification live cell imaging during cell stretching. While a uniaxial system was recently described that also achieved this task (Gerstmair et al. 2009), we present for the first time a system that is able to image cells anywhere on a substrate that is undergoing a biaxial strain, enabling and facilitating multiple single cell measurement within a given experiment.

Cellular experiments were performed using a known osteoblastic model (SAOS-2) (Mayr-Wohlfart et al. 2001; Li et al. 2006) and the platform was demonstrated to be able to discern different cell stiffness based on resistance to substrate deformation. Furthermore the results reflect similar trends shown by the atomic force microscopy experiments used here as a benchmark. AFM indentation gives information about cellular mechanical behavior in response to localized compression (differing from the tensile load applied by our platform) that may be useful for assessing cell membrane bending resistance or cytosolic stiffness, but is of questionable relevance for assessing the fibrous elements of the actin cytoskeleton. However, we hypothesized that the tensile and compressive techniques would show a similar trend with respect to the different chemical treatments applied (Cytochalasin-D and Glutaraldehyde), and therefore we presented these experiments as a "gold standard" for characterization of cell stiffness. While the cell stiffness trends were confirmed using the novel tensile assay, the large difference shown in AFM experiments between Glutaraldehyde-treated cells and untreated cells was not reflected in the strain patterns and strain drop (which only doubled in the tensile experiment compared to order of magnitude differences in compression). This phenomenon reflects the non-linear response of our platform which was tuned (by strategic choice of the interpositional PDMS cell substrate stiffness) to be sensitive to a certain cell stiffness range. If it is the goal to discern cells of higher stiffness than 5 kPa, accordingly stiffer PDMS layers can be applied.

The method we introduce has some limitations. Experimental outcomes using the novel configuration of an interpositional soft PDMS gel between cells and the standard FlexCell silicone membranes (Fig. 7) differed slightly from analogous finite element predictions (Fig. 3). In particular it is clear that the central symmetry simulated in the FE models was not reflected in the experiments,

which rather showed some cell polarity with anisotropic strain distributions. Factors such as cell anisotropy, discrete focal adhesion distribution and associated actin stress fibers, none of which were modeled here for simplicity, likely contribute to this discrepancy. The models were further simplified in the assumed isotropic and linear elastic material model, while it is known that the cell material behavior is rather viscoelastic and anisotropic (Zhu et al. 2000; Stamenovic ‡ 2008). Furthermore the cells were modeled as being bound to the substrate over their entire footprint, while it is known that cells adhere by binding at discrete and dynamic focal adhesions (Dembo and Wang 1999). Nonetheless, consistency in cell morphology before and after the applied cell stretch (data not shown) did lead us to assume that the cell-substrate bond was relatively stable over the course of the experiment.

Modeling individual focal adhesions and pre-stressed actin bundles are likely to improve bio-fidelity and accuracy of the model, and improvement in the finite element model and its application in an inverse approach to more precisely quantify cell constitutive properties does represent a key next step. This would enable an absolute quantification of stiffness to be assigned to each tested cell. At the same time, the non-symmetric strain patterns found in the experimental results could potentially be exploited to investigate aspects of anisotropic cellular mechanical behavior.

Another limitation is inherent in the use of a 2D substrate, which is by now widely known to result in cellular behaviors different from the 3D physiological environment. Attempts of embedding cells in three-dimensional matrix such as Matrigel or fibronectin (Mao and Schwarzbauer 2005) can be found in the literature, and this is being integrated into our platform as a thin quasi-3D layer. Such efforts are complicated by difficulties in applying an appropriate interpretation of the cell-matrix interaction, and extension of the platform to the third dimension will require a more sophisticated image analysis approach (Graf and Boppart 2010).

Cell-substrate attachment, number and dimension of focal adhesions, and cell orientation could also limit the consistency of the outcome influencing the strain imparted to the cell and thus its apparent resistance to stretch (Barbee et al. 1994; Smith et al. 1997; Wall et al. 2007), as measured by our platform. However, our results showed that a decrease in cell stiffness was mirrored in a pronounced drop in ability to resist the applied substrate deformation, although some variation within the tested cell populations was observed.

Manual focus readjustment also represents a limitation with respect to the speed of the stretching experiment. Automatic compensation of the stage along the z-axis will address this problem and allow faster experiments (<1 s) leading, along with cells expressing EGFP-tagged F-actin (and/or focal adhesion proteins), to the investigation of real-time cytoskeleton rearrangement under stretch.

In conclusion, a novel functional imaging platform has been designed and implemented that brings together interesting features: (a) cell stretch is over a range of 0–8%; (b) substrate stiffness is tunable thus allowing corresponding sensitivity tuning and investigation of various cell types, but also the possibility to mimic different types of extracellular ligand; (c) the addition of an interpositional substrate has been demonstrated not to alter the strain field imposed by the commercial actuator; (d) the tracking and stage compensation system has been shown to be able to keep single cells centered within the microscope field of view while the cell is being stretched; (e) the strain calculation algorithm based on DIC was shown to be fast, accurate, and reliable in quantifying the strain field between a reference and a deformed image.

The functional imaging platform we introduce could represent a useful tool for basic research into single-cell mechanical properties as a function of both substrate mechanics (passive and active) and surface chemistry (although only one ligand type and loading was investigated here). To our knowledge, it also represents a unique technical system enabling high magnification, single cell characterization of dynamic cytoskeletal response to mechanical substrate actuation, and could represent a viable platform for providing substrate actuation to coupled PDMS micro-devices.

Acknowledgments The authors gratefully acknowledge Professor Janos Vörös for use of the AFM. We also thank Mr. Hansruedolf Sommer for his contribution to device construction, and Pascal Bissig and Michael Bieri from the ETH Zurich for their contribution to the tracking system design and implementation.

This study was funded by the Swiss National Science Foundation, grant number 205321-118036.

References

I. Arganda-Carreras, C.O.S. Sorzano et al., Consistent and elastic registration of histological sections using vector-spline regularization. Comput Vis Approaches Med Image Anal **4241**, 85–95 (2006)

K.A. Barbee, E.J. Macarak et al., Strain measurements in cultured vascular smooth muscle cells subjected to mechanical deformation. Ann Biomed Eng **22**(1), 14–22 (1994)

F.H. Bieler, C.E. Ott et al., Biaxial cell stimulation: A mechanical validation. J Biomech **42**(11), 1692–1696 (2009)

S.Y. Chou, C.M. Cheng et al., Composite polymer systems with control of local substrate elasticity and their effect on cytoskeletal and morphological characteristics of adherent cells. Biomaterials **30**(18), 3136–3142 (2009)

S.E. Cross, Y.S. Jin et al., Nanomechanical analysis of cells from cancer patients. Nat Nanotechnol **2**(12), 780–783 (2007)

S.E. Cross, Y.S. Jin, et al. AFM-based analysis of human metastatic cancer cells. Nanotechnology. **19**(38), (2008)

E.M. Darling, S. Zauscher et al., A thin-layer model for viscoelastic, stress-relaxation testing of cells using atomic force microscopy: Do cell properties reflect metastatic potential? Biophys J **92**(5), 1784–1791 (2007)

M. Dembo, Y.L. Wang, Stresses at the cell-to-substrate interface during locomotion of fibroblasts. Biophys J **76**(4), 2307–2316 (1999)
E.K. Dimitriadis, F. Horkay et al., Determination of elastic moduli of thin layers of soft material using the atomic force microscope. Biophys J **82**(5), 2798–2810 (2002)
D. Docheva, D. Padula et al., Researching into the cellular shape, volume and elasticity of mesenchymal stem cells, osteoblasts and osteosarcoma cells by atomic force microscopy. J Cell Mol Med **12**(2), 537–552 (2008)
A.J. Foulkes, R.C. Miall, Adaptation to visual feedback delays in a human manual tracking task. Exp Brain Res **131**(1), 101–110 (2000)
A. Gerstmair, G. Fois et al., A device for simultaneous live cell imaging during uni-axial mechanical strain or compression. J Appl Physiol **107**(2), 613–620 (2009)
B.W. Graf, S.A. Boppart, Imaging and analysis of three-dimensional cell culture models. Methods Mol Biol **591**, 211–227 (2010)
J. Guck, S. Schinkinger et al., Optical deformability as an inherent cell marker for testing malignant transformation and metastatic competence. Biophys J **88**(5), 3689–3698 (2005)
J.H. Hoh, C.A. Schoenenberger, Surface morphology and mechanical properties of MDCK monolayers by atomic force microscopy. J Cell Sci **107**(Pt 5), 1105–1114 (1994)
R. Krishnan, C.Y. Park et al., Reinforcement versus fluidization in cytoskeletal mechanoresponsiveness. PLoS ONE **4**(5), e5486 (2009)
G.Y. Lee, C.T. Lim, Biomechanics approaches to studying human diseases. Trends Biotechnol **25**(3), 111–118 (2007)
C.Y. Li, S.Y. Gao et al., In vitro assays for adhesion and migration of osteoblastic cells (Saos-2) on titanium surfaces. Cell Tissue Res **324**(3), 369–375 (2006)
C.T. Lim, E.H. Zhou et al., Mechanical models for living cells—A review. J Biomech **39**(2), 195–216 (2006)
B. Lincoln, H.M. Erickson et al., Deformability-based flow cytometry. Cytom A **59**(2), 203–209 (2004)
B. Lincoln, S. Schinkinger et al., Reconfigurable microfluidic integration of a dual-beam laser trap with biomedical applications. Biomed Microdevices **9**(5), 703–710 (2007)
Y. Mao, J.E. Schwarzbauer, Stimulatory effects of a three-dimensional microenvironment on cell-mediated fibronectin fibrillogenesis. J Cell Sci **118**(Pt 19), 4427–4436 (2005)
T. Masuda, I. Takahashi et al., Development of a cell culture system loading cyclic mechanical strain to chondrogenic cells. J Biotechnol **133**(2), 231–238 (2008)
U. Mayr-Wohlfart, J. Fiedler et al., Proliferation and differentiation rates of a human osteoblast-like cell line (SaOS-2) in contact with different bone substitute materials. J Biomed Mater Res **57**(1), 132–139 (2001)
S. Munevar, Y.L. Wang et al., Traction force microscopy of migrating normal and H-ras transformed 3T3 fibroblasts. Biophys J **80**(4), 1744–1757 (2001)
T. Ochalek, F.J. Nordt et al., Correlation between cell deformability and metastatic potential in B16-F1 melanoma cell variants. Cancer Res **48**(18), 5124–5128 (1988)
A.A. Patel, R.G. Thakar et al., Biophysical mechanisms of single-cell interactions with microtopographical cues. Biomed Microdevices **12**(2), 287–296 (2010)
M. Paulitschke, G.B. Nash, Membrane rigidity of red-blood-cells parasitized by different strains of plasmodium-falciparum. J Lab Clin Med **122**(5), 581–589 (1993)
D.B. Serrell, T.L. Oreskovic et al., A uniaxial bioMEMS device for quantitative force-displacement measurements. Biomed Microdevices **9**(2), 267–275 (2007)
D. Shin, K. Athanasiou, Cytoindentation for obtaining cell biomechanical properties. J Orthop Res **17**(6), 880–890 (1999)
P.G. Smith, R. Garcia et al., Strain reorganizes focal adhesions and cytoskeleton in cultured airway smooth muscle cells. Exp Cell Res **232**(1), 127–136 (1997)
J.G. Snedeker, G. Pelled et al., Endoscopic cellular microscopy for in vivo biomechanical assessment of tendon function. J Biomed Opt **11**(6), 064010 (2006)
D. Stamenovic ‡, Rheological behavior of mammalian cells. Cell Mol Life Sci **65**(22), 3592–3605 (2008)
S. Suresh, Biomechanics and biophysics of cancer cells. Acta Biomater **3**(4), 413–438 (2007)
S. Suresh, J. Spatz et al., Connections between single-cell biomechanics and human disease states: gastrointestinal cancer and malaria. Acta Biomater **1**(1), 15–30 (2005)
J.L. Tan, J. Tien et al., Cells lying on a bed of microneedles: an approach to isolate mechanical force. Proc Natl Acad Sci USA **100**(4), 1484–1489 (2003)
W. Tan, T.A. Desai, Layer-by-layer microfluidics for biomimetic three-dimensional structures. Biomaterials **25**(7–8), 1355–1364 (2004)
J.P. Vande Geest, E.S. Di Martino et al., An analysis of the complete strain field within Flexercell membranes. J Biomech **37**(12), 1923–1928 (2004)
B. Wacogne, C. Pieralli et al., Measuring the mechanical behaviour of human oocytes with a very simple SU-8 micro-tool. Biomed Microdevices **10**(3), 411–419 (2008)
M.E. Wall, P.S. Weinhold et al., Comparison of cellular strain with applied substrate strain in vitro. J Biomech **40**(1), 173–181 (2007)
Y.L. Wang, R.J. Pelham Jr., Preparation of a flexible, porous polyacrylamide substrate for mechanical studies of cultured cells. Methods Enzymol **298**, 489–496 (1998)
P.J. Wipff, H. Majd et al., The covalent attachment of adhesion molecules to silicone membranes for cell stretching applications. Biomaterials **30**(9), 1781–1789 (2009)
W.J. Yao, L. Gu et al., Wild type p53 gene causes reorganization of cytoskeleton and, therefore, the impaired deformability and difficult migration of murine erythroleukemia cells. Cell Motil Cytoskeleton **56**(1), 1–12 (2003)
C. Zhu, G. Bao et al., Cell mechanics: mechanical response, cell adhesion, and molecular deformation. Annu Rev Biomed Eng **2**, 189–226 (2000)